Electronic Supplementary Material (ESI) for Physical Chemistry Chemical Physics.
This journal is © the Owner Societies 2014

SUPPORTING INFORMATION

Improved Efficiency for Bulk Heterojunction Hybrid Solar Cells by utilizing CdSe Quantum Dot - Graphene Nanocomposites

*Michael Eck[a,b], Chuyen Van Pham[a,b], Simon Züfle[c,d], Martin Neukom[d], Martin Sessler[a,e], Dorothea Scheunemann[g], Emre Erdem[f], Stefan Weber[f], Holger Borchert[g], Beat Ruhstaller[c,d], Michael Krüger[a,b]**

[a]*Freiburg Materials Research Center (FMF), University of Freiburg, Stefan-Meier-Straße 21, D-79104 Freiburg, Germany.*

[b]*Department of Microsystems Engineering (IMTEK), University of Freiburg, Georges-Köhler-Allee 103, D-79110 Freiburg, Germany*

[c]*Institute of Computational Physics, Zurich University of Applied Sciences (ZHAW), Technikumstrasse 9, CH-8401 Winterthur, Switzerland*

[d]*Fluxim AG, Technoparkstrasse 2, CH-8406 Winterthur, Switzerland*

[e]*Fraunhofer Institute for Solar Energy Systems (ISE), Heidenhofstraße 2, D-79110 Freiburg, Germany*

[f]*Institute of Physical Chemistry, University of Freiburg, Albertstraße 21, D-79104 Freiburg, Germany*

[g]*Department of Physics, Carl von Ossietzky University of Oldenburg, Carl-von-Ossietzky-Straße 9-11, D-26129 Oldenburg, Germany*

TrGO dispersion:

SEM images of particles contained in the TrGO dispersion ($c \leq 50$ µg/ml) (Fig. S1a) are shown in Fig. S1b,c. The images reveal a wide size distribution of the TrGO sheets. Some sheets exhibit sizes of over 1 µm down to 80 nm or smaller. There are also large aggregates of about 10 µm observable composed out of sheets with about 1 µm in diameter.

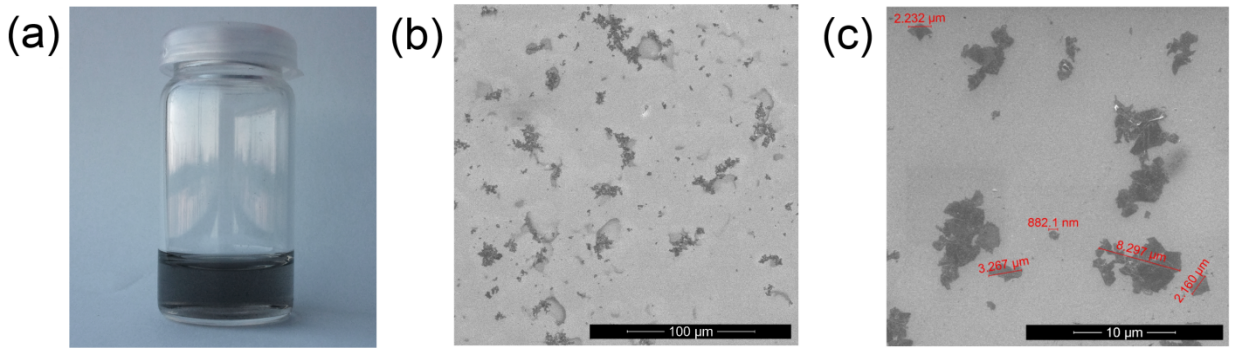

Figure S1. (a) 12 h reduced and thiol-functionalized TrGO with a concentration of <50 µg/ml in DMF after waiting one day for the fallout of large, indispersable TrGO aggregates. (b) Scanning electron microscopy (SEM) image of the same TrGO solution drop-casted on an ITO (c) zoomed SEM image reveals diameters of the TrGO particles of a wide range between ca. 3 µm down to under 80 nm. Larger particles seem to be composed out of aggregated sheets of about 1µm in length.

Absorption and photoluminescence of CdSe-TrGO hybrid:

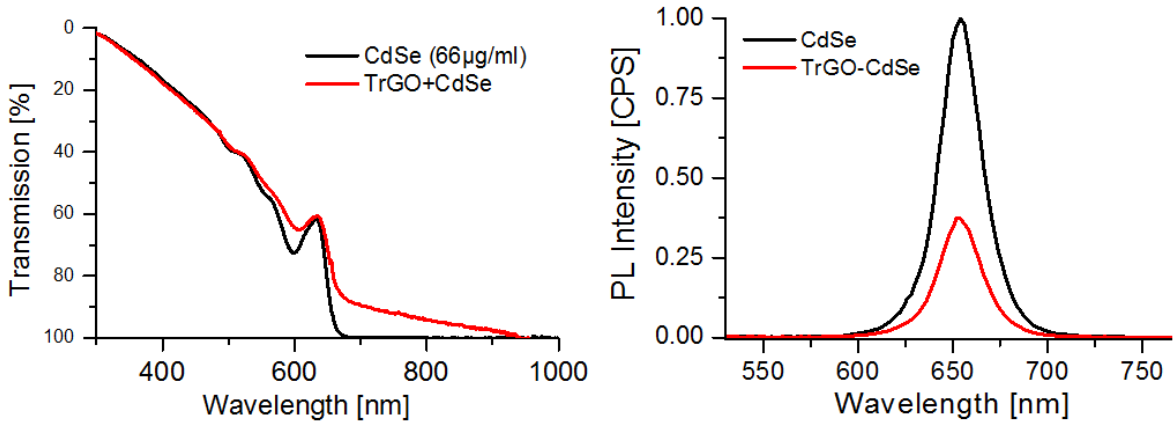

Figure S2. Left: Transmission spectra of a 66 µg/ml dispersion of CdSe NCs in $CHCl_3$ and of a mixture between CdSe of the same concentration and TrGO of 0.66µg/ml DMF. Right: PL spectra of the same two solutions directly after mixing.

Absorption of polymer-TrGO mixture:

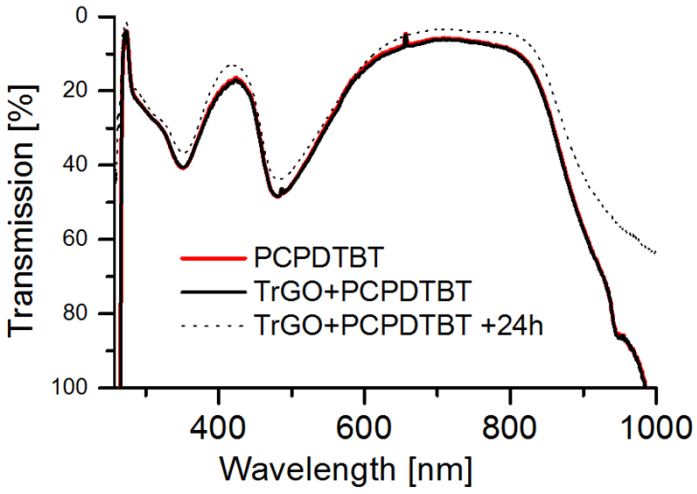

Figure S3. Transmission spectra of a PCPDTBT solution in $CHCl_3$ and of a mixture between PCPDTBT in $CHCl_3$ and TrGO in DMF, both directly after mixing and 24 hours later.

Scanning electron microscopy images of the active layer surface:

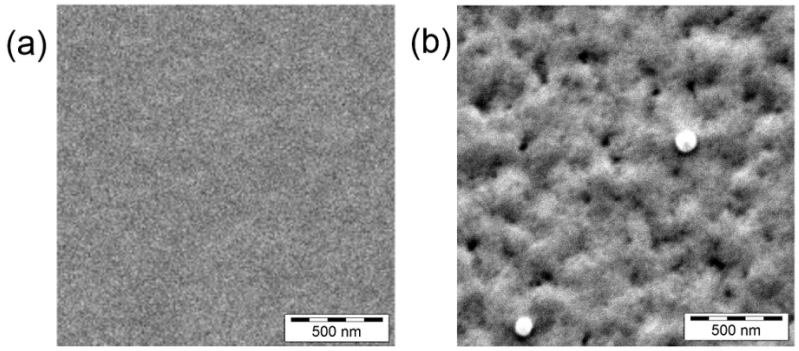

Figure S4. a): Scanning electron microscopy (SEM) images of the active layer surface of a CdSe/PCPDTBT and b): of a TrGO-CdSe/PCPDTBT solar cell. The observable white spots are probably dust particles, occasionally observable also on the TrGO free solar cell.

Slices in parallel to the active layer from the electron tomography analysis:

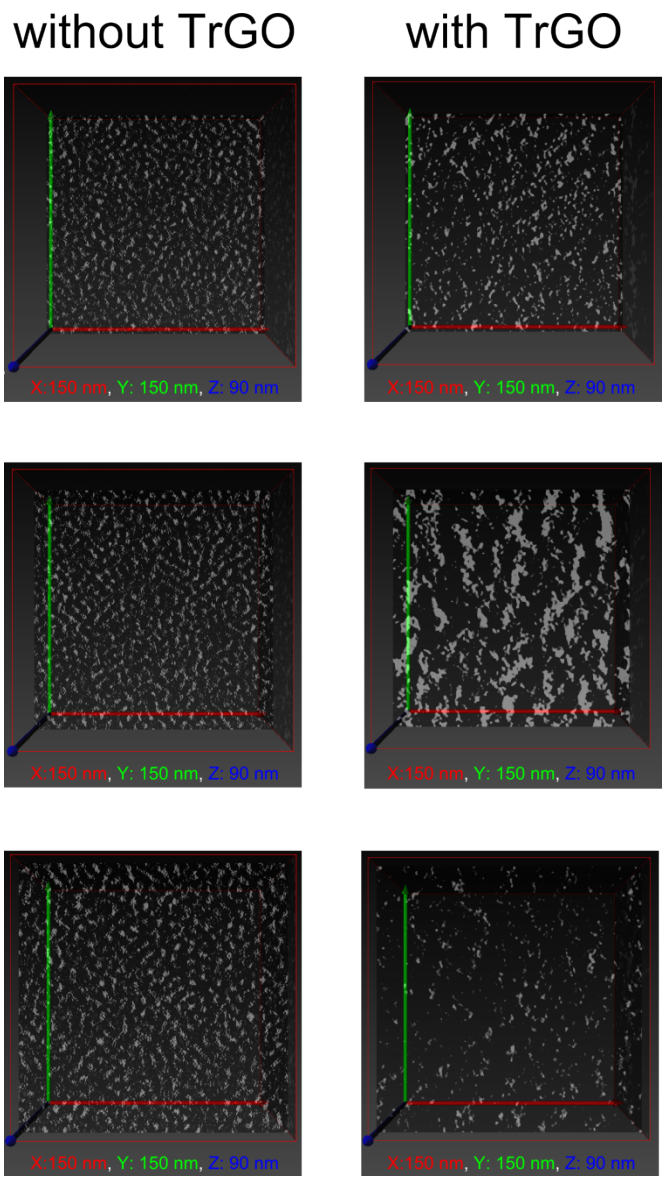

Figure S5. Slices through the reconstructed volume of active layers isolated from solar cells without TrGO (left column) and with TrGO (right column). For both cases, three slices parallel to the x-y plane (i.e., parallel to the active layer) are shown, corresponding to different positions

in the z-direction (images in the middle line: in the middle of the active layer; upper images: closer to the ITO/PEDOT:PSS anode; bottom images: closer to the metal cathode). Without TrGO, the CdSe nanocrystals appear to be rather homogeneously distributed throughout the active layer. In contrast, with TrGO, the phase separation is significantly coarser in all regions of the film. Furthermore, regarding the distribution of the material along the z-axis, the concentration of CdSe seems to be enriched in the middle of the active layer.

Influence of CdSe:polymer ratio on the solar cell performance:

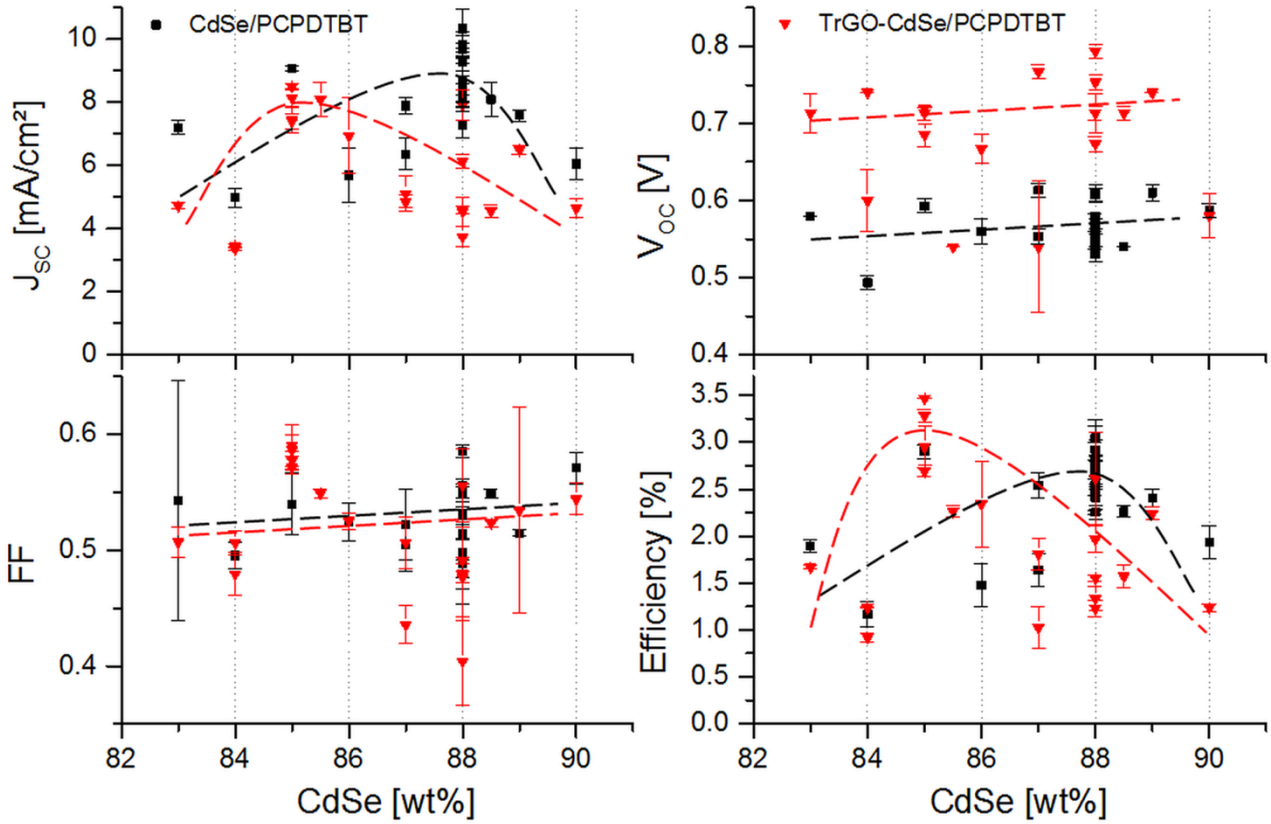

Figure S6. Short-circuit current density, fill factor, open-circuit voltage and power conversion efficiency from 19 CdSe/PCPDTBT and 19 TrGO-CdSe/PCPDTBT devices with 3 individual solar cells on each. The data points represent the average value of each device, bars represent the value range of the respective device. All cells were measured under a sun simulator without

spectral mismatch correction at 100 mW/cm². An active area of 0.065 cm² was assumed. Dashed trend lines are inserted for easier visualization for both solar cell types (red dashed for CdSe/PCPDTBT and black dashed for TrGO-CdSe/PCPDTBT).

The relatively large fluctuations in the V_{OC} when taking in account all 114 measured individual solar cells of up to ± 0.075 V - even if repeating experiments of the same CdSe/polymer ratio - might be explained by a different degree of aggregation of the NCs in the ink prior to their spin coating[S1]. Deriving from slightly different times the QDs were kept after the post synthetic treatment in solution, and additionally by a different aggregation degree resulting already from the prior postsynthetic ligand removal procedure. Observed fluctuations of the J_{SC}, even for the same NC:polymer ratio, might largely be attributed to variation of the real solar cell active area induced by the manufacturing process.

Table S1. Average device parameters and standard deviations from a total of 42 CdSe/PCPDTBT and TrGO-CdSe/PCPDTBT solar cells manufactured in the optimum CdSe QD:polymer ratio, measured in our laboratory with a sun simulator at 100 mW/cm², without consideration of spectral mismatch and an assumed active area of 0.65 cm². The values for the two outer and the inner solar cells are given separately.

		J_{SC} [mA/cm²]	FF	V_{OC} [V]	PCE [%]
CdSe/PCPDTBT	outer solar cells	9.01	0.549	0.569	2.71
	(std. dev.)	1.13	0.049	0.027	0.35
	inner solar cell	8.84	0.536	0.566	2.59
	(std. dev.)	0.66	0.060	0.023	0.23
TrGO-CdSe/PCPDTBT	outer solar cells	8.21	0.576	0.713	3.26
	(std. dev.)	0.65	0.014	0.010	0.33

inner solar cells	7.74	0.592	0.715	3.08
(std. dev.)	0.65	0.019	0.010	0.35

Internal quantum efficiency comparison:

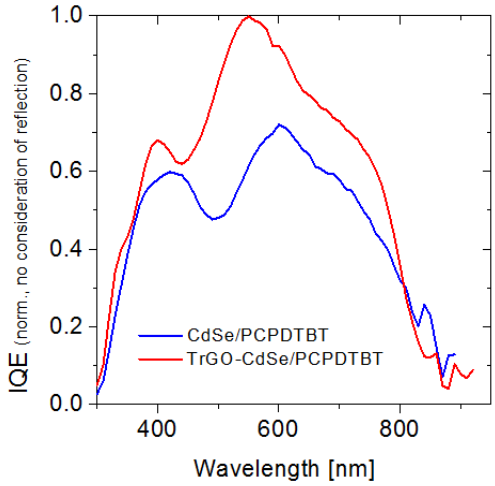

Figure S7. Normalized internal quantum efficiency (IQE) for both solar cell types, obtained by calculating the quotient between the respective percentage of the EQE and absorption spectrum of the active layer, without consideration of the reflection spectrum.

From Figure 7b in the main text one can see that the TrGO containing cell exhibits a much lower CdSe absorption, observable from the less prominent absorption peak at 640 nm and a lower absorption at wavelengths below, which can be explained by the observed stronger QD aggregation in the active layer. On the other hand, the polymer absorption is only slightly stronger, observable from a higher absorption over 650 nm, also deriving from the slightly higher polymer fraction used for the optimized TrGO-CdSe/polymer solar cell. The resulting EQE (Fig. 7a, main text) demonstrates a much higher current output per incident photons for wavelengths between 500-800 nm, a region of strong polymer absorption. Given the only slightly higher polymer absorption, the resulting IQE - without consideration of reflection - (see Fig. S7) is therefore considerably higher in this region. This demonstrates a superior extraction of electrons

excited in the polymer phase for the TrGO containing solar cells, with the CdSe QDs apparently contributing less to the photocurrent generation compared to the TrGO free solar cell.

Device performance measured at the group for dye and organic solar cells of the Fraunhofer ISE:

Table S2. Device parameters measured at the Fraunhofer ISE of each pixel of CdSe/PCPDTBT and TrGO-CdSe/PCPDTBT solar cells 20 days after their manufacturing.

		area [cm²]	J_{SC} [mA/cm²]	FF	V_{OC} [V]	PCE [%]
CdSe/PCPDTBT	cell1	0.0595	8.956	0.566	0.554	2.913
	cell2	0.0630	8.811	0.563	0.562	2.894
	cell3	0.0610	8.558	0.569	0.553	2.689
	average	0.0612	8.775	0.566	0.556	2.832
	+/-	0.0018	0.199	0.003	0.005	0.112
TrGO-CdSe/PCPDTBT	cell1	0.0576	10.275	0.547	0.720	4.045
	cell2	0.0540	8.832	0.563	0.718	3.567
	cell3	0.0517	10.740	0.548	0.721	4.244
	average	0.0544	9.949	0.553	0.720	3.952
	+/-	0.0030	0.954	0.008	0.002	0.338

CELIV measurements:

The cells used for the CELIV measurements (Fig. S8) were sealed against degradation on air for transportation to FLUXIM AG with a 1 mm thick glass plate over the active layer, fixed to the cell by melting for 3min at 145°C of a 25µm thick Solaronix thermoplastic sealing film.

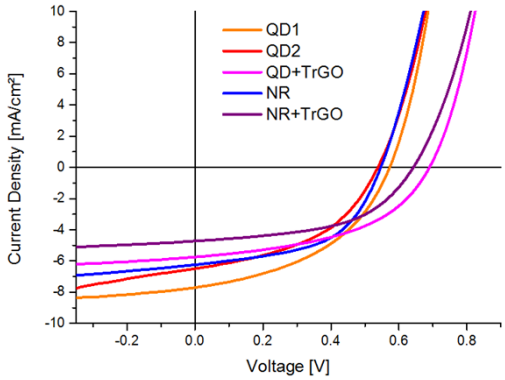

Figure S8. J-V curves of the solar cells used for CELIV at FLUXIM AG with active layers from a 88:12 weight ratio of CdSe quantum dot (QD):PCPDTBT (2 cells), TrGO-CdSe QD:PCPDTBT, CdSe nanorod (NR):PCPDTBT, and TrGO-CdSe NR:PCPDTBT after sealing.

During the CELIV measurement (see Fig. S9) a voltage ramp (here 400 mV/µs) in reverse bias is applied to the solar cell. Extracted charges are visible as a current in an external sensing circuit.

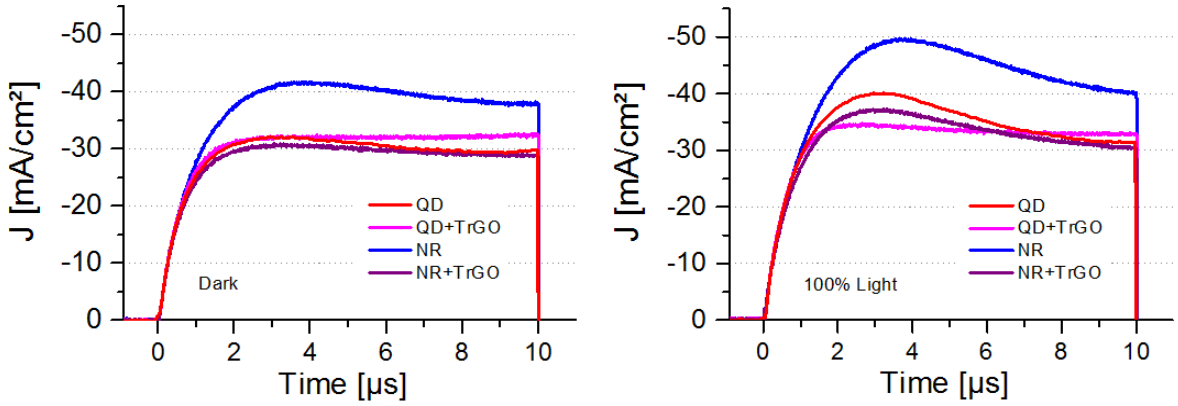

Figure S9. CELIV currents of CdSe/polymer and TrGO-CdSe/polymer solar cells from CdSe QDs and NRs under illumination and in the dark.

From the time t_{max} of the current peak one can calculate the mobility µ of the fastest charge carrier. In case that the current density caused by the geometric capacitance of the solar cell $j(0)$ is in a similar range as the maximum of the extracted current density Δj the following formula can be applied:

with d being the thickness of the active layer and A being the applied voltage slope.

The current density due to the capacitive response *j(0)* of the solar cell can be calculated as follows

and then subtracted from the measured current density j to obtain Δj, which is representing the actual targeted current density to measure. So, one has to first obtain the capacity C of the solar cell to make a statement about the mobility. However, only in case that hole mobility μ_h and electron mobility μ_e would be very different from each other and the number of both positive and negative charges being similar, both current peaks would be visible during the extraction. But, if both mobilities are in a similar range, one will not be able to distinguish between the charge carriers. In our measurements of the fresh cells there is also only one peak observable, but from repeating the CELIV measurement over several days during the degradation of the solar cell on air, one can notice two peaks forming (see Fig.S10), with the later one increasing by time, which is attributed to the presumably lower electron mobility, therefore exhibiting an n-doping in the CdSe/polymer solar cell during degradation.

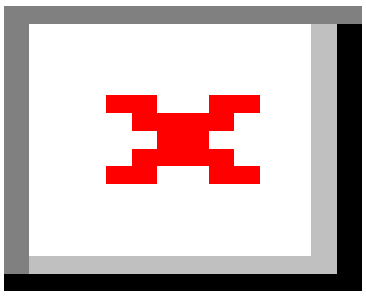

Figure S10. CELIV measurement of a CdSe QD/polymer solar cell during its degradation. An additional second peak emerges, which is attributed to the presumably slower electrons. Thereby, by with degradation a n-doping of the solar cell is occurring.

With this finding one can identify both the position for the hole and for the electron extraction peak from the CELIV measurements of the fresh cells. In order to extract the geometrical capacitance of the solar cells, impedance spectroscopy (IS) measurements were performed (see Fig. S11).

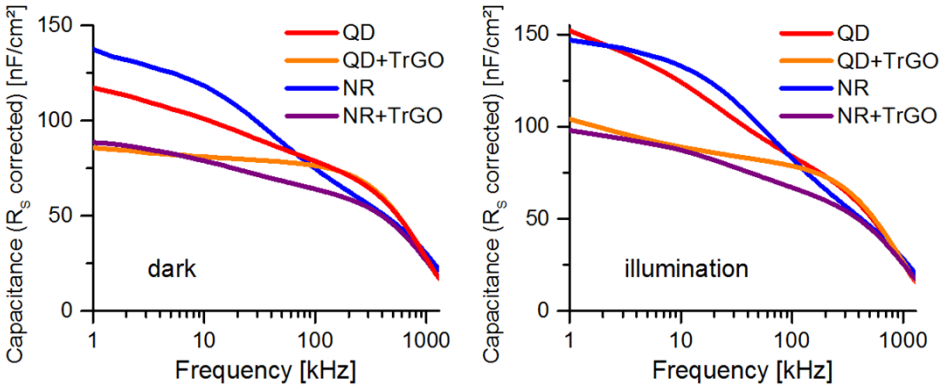

Figure S11. Capacitance density vs. frequency plots of CdSe/polymer and TrGO-CdSe/polymer solar cells from CdSe QDs and NRs in dark and under illumination.

However, in absence of a plateau area, one was not able to extract the geometrical capacitance from IS. Therefore, a capacitance-voltage measurement was performed (see Fig. S12) by applying DC offset voltage between -2 V and 1.5 V to a 10 kHz AC signal. The thereby extracted values for the capacitance, built in voltage, relative permittivity ε_r, and *j(0)* are listed in Table S2.

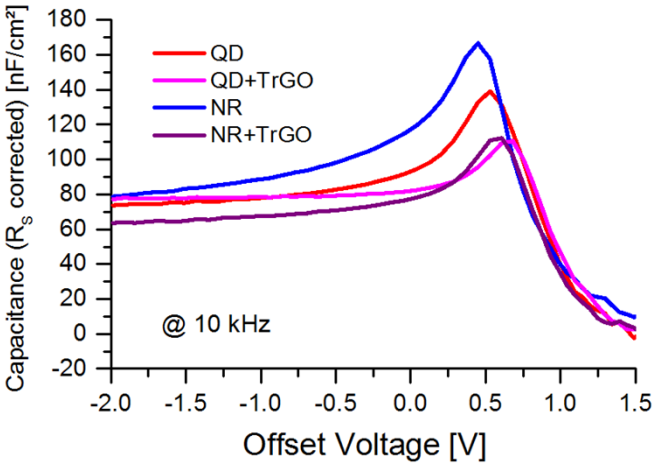

Figure S12. Capacitance vs. DC offset voltage at a modulation frequency of 10 kHz for the CdSe QD/PCPDTBT, TrGO-CdSe QD/PCPDTBT, CdSe NR/PCPDTBT, and TrGO-CdSe NR/PCPDTBT solar cell respectively.

Table S3. Extracted values for the capacitance-density, built in voltage (V_{bi}), relative permittivity (ε_r), and j(0) from the capacitance-voltage measurement at 10 kHz, for an active layer thickness of 80 nm.

	***C* [nF/cm²]**	***V_{bi}*[eV]**	***ε_r***	***j(0)* [mA/cm²]**
QD	74	0.53	6.69	29.6
QD+TrGO	77	0.68	6.96	30.8
NR	79	0.45	7.14	31.6
NR+TrGO	64	0.59	5.78	25.6

Table S4. Electron and hole mobilities extracted from CELIV measurements for CdSe NR/PCPDTBT and TrGO-CdSe NR/PCPDTBT solar cells.

	***μ_e* [cm²/Vs]**	***μ_h* [cm²/Vs]**
CdSe/PCPDTBT	0.9×10^{-5}	8×10^{-5}
TrGO CdSe/PCPDTBT	1.5×10^{-5}	

Dark current of CdSe/polymer and of TrGO-CdSe/polymer solar cells:

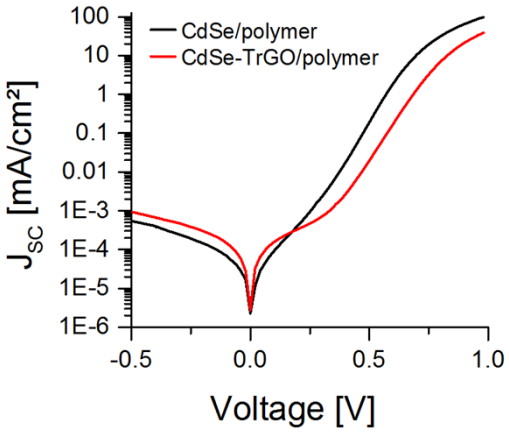

Figure S13. Dark current density vs. voltage for a solar cell from a CdSe QD/PCPDTBT and a CdSe QD-TrGO/PCPDTBT solar cell.

Light intensity dependency of V_{OC}:

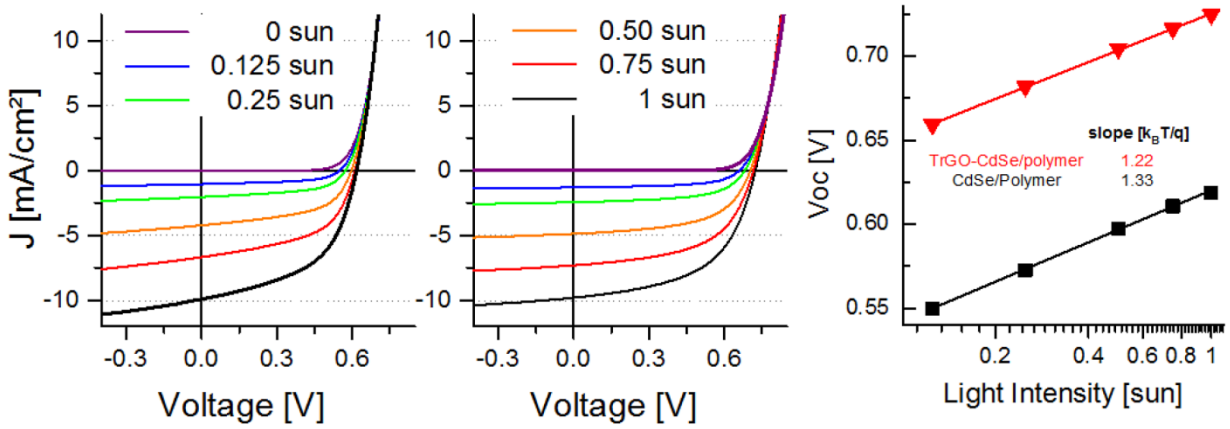

Figure S14. Dependence of the open-circuit voltage on the illumination intensity in a CdSe/PCPDTBT solar cell (left) and in a TrGO-CdSe/PCPDTBT solar cell (middle). The resulting slope of the V_{OC} vs. the light intensity results in the ideality factor of the respective solar cell (right).

PCBM/polymer solar cells with and without addition of TrGO:

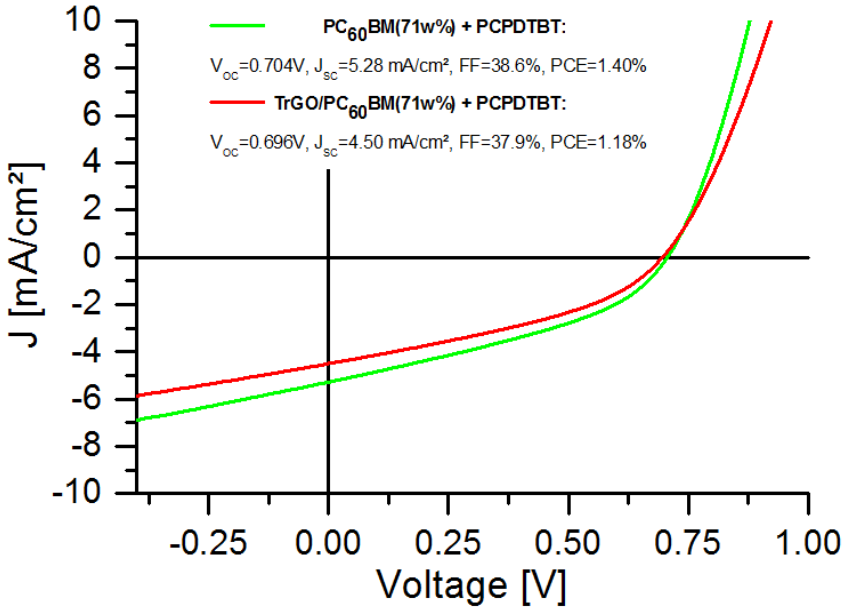

Figure S15. Current density vs. voltage for a solar cell from $PC_{60}BM$/PCPDTBT and a $PC_{60}BM$/TrGO/PCPDTBT solar cell.

REFERENCE:

S1 M. Schubert, D. Dolfen, J. Frisch, S. Roland, R. Steyrleuthner, B. Stiller, Z. Chen, U. Scherf, N. Koch, A. Facchetti and D. Neher, *Adv. Energ. Mater.*, 2012, **2**, 369–380.